THE ANNALS OF "DUNĂREA DE JOS" UNIVERSITY OF GALAȚI
FASCICLE V, TECHNOLOGIES IN MACHINE BUILDING,
ISSN 1221- 4566, 2011

SURFACE PROFILING METHOD OF THE DISK CUTTER OF THE MALE ROTOR FROM THE SCREW COMPRESSOR COMPONENT

Camelia Popa, Virgil Teodor, Ionuț Popa, Nicolae Oancea

"Dunărea de Jos" University of Galați
virgil.teodor@ugal.ro

ABSTRACT

The active surfaces of the screw compressors rotors are cylindrical helicoidal surfaces, with constant step; these surfaces are complex surfaces in order to meet a set of specifics conditions.

This paper presents, according to the theorems referring to enveloping surfaces, a specific application regarding the principle of replacement of elementary generators surfaces belonging to the set of helicoidal surfaces described by dot matrix, using the tangent method , in order to determine the shape of disk cutter profile for the male rotor. Also, based on a Java soft product, we present frontal applications of the axial shapes of the generating disk cutter for the male rotor, component of screw compressor, gear ratio 4/6 and 3/5.

KEYWORDS: helicoidal surfaces, Bézier polynomial, meshing surfaces, disk cutter

1. Introduction

The screw compressor rotors profiling (in cross section), starts with the rack generating [6], according to the enveloping method [1], [2], in order to determine, analytically or numerical, by these shapes.

Once known the shape in cross section, we can get the transverse profile of the meshing rotor [7], [8], [9], [10] solving the problem as a matter of enveloping with plane profiles belonging to one couple of centrodes.

The enveloping surfaces study can be done based on the fundamental theorems of enveloping surfaces, Olivier and Gohman theorems [1]; we can also use one of complementary theorems: "The minimum distance method" [3] and "The substitutive circles family" [3], or "The method of plane trajectory generation" [4]. The graphics methods 2D or 3D can solve the problem also [5], [6], [13].

The screw compressor active surfaces can be manufactured using the disk cutter, whose primary peripheral surfaces are revolution ones conjugated with rotors helical surfaces.

2. The helical surfaces of male rotor

The coordinates system attached to disk cutter and its circular centrode are defined in Figure 1. Table 1 presents the profiles of the generating rack for the system $\xi\eta$.

The cinematic process of generation means the rolling of the two centrodes: one linear C, of the rack, the other one circular, C1, radius Rr1, specific to cross section of the male rotor.

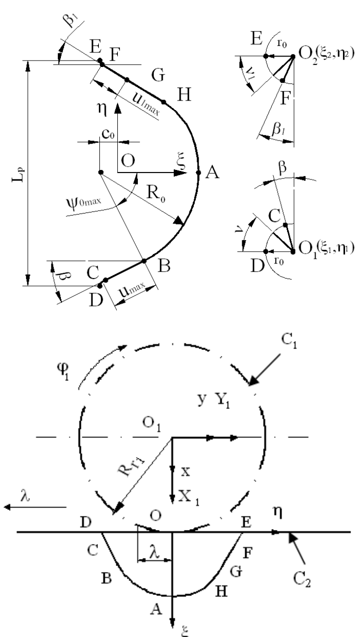

Fig. 1. *Rolling centrodes; male rotor profiling*

In Table 2, we present the analytic models of transverse section of male rotor (family of plane profiles and meshing conditions).

Table 1. *The rack profiles*

Sg.	Profiles	Variable parameters
$\overset{\frown}{AB}$	$\begin{cases}\xi(\psi)=R_0\cdot\cos\psi-c_0;\\ \eta(\psi)=-R_0\cdot\sin\psi.\end{cases}$	$\psi_{min}=0$; ψ_{max} - constructive
$\overline{BC}$	$\begin{cases}\xi(u)=\xi_B-u\cdot\cos\beta;\\ \eta(u)=\eta_B-u\cdot\sin\beta.\end{cases}$	$u_{min}=0$; u_{max} - contructive $\beta=\frac{\pi}{2}-\psi_{max}$
$\overset{\frown}{CD}$	$\begin{cases}\xi(\nu)=-r_0\cdot\cos\nu+\xi_{0_1};\\ \eta(\nu)=+r_0\cdot\sin\nu+\eta_{0_1}.\end{cases}$	$\upsilon_{min}=0$; $\upsilon_{max}=\frac{\pi}{2}-\beta$
$\overset{\frown}{EF}$	$\begin{cases}\xi(\nu_1)=-r_0\cdot\cos\nu_1+\xi_{0_2};\\ \eta(\nu_1)=-r_0\cdot\sin\nu_1+\eta_{0_2}.\end{cases}$	$\upsilon_{1min}=0$; $\upsilon_{1max}=\frac{\pi}{2}-\beta_1$
$\overline{FG}$	$\begin{cases}\xi(u_1)=+u_1\cdot\cos\beta_1+\xi_F;\\ \eta(u_1)=-u_1\cdot\sin\beta_1+\eta_F.\end{cases}$	$u_{1min}=0$; u_{1max}=constructive
$\overset{\frown}{AH}$	$\begin{cases}P_{\xi AH}=\lambda_1^2A_\xi+2(1-\lambda_1)\lambda_1B_\xi+(1-\lambda_1)^2C_\xi;\\ P_{\eta AG}=\lambda_1^2A_\eta+2(1-\lambda_1)\lambda_1B_\eta+(1-\lambda_1)^2C_\eta,\end{cases}$	$0\le\lambda_1\le1$
$\overset{\frown}{GH}$	$\begin{cases}P_{\xi HG}=\lambda_2^2D_\xi+2(1-\lambda_2)\lambda_2E_\xi+(1-\lambda_2)^2F_\xi;\\ P_{\eta HG}=\lambda_2^2D_\eta+2(1-\lambda_2)\lambda_2E_\eta+(1-\lambda_2)^2F_\eta,\end{cases}$	$0\le\lambda_2\le1$

The transverse profiles of male rotor, see Figure 1, can be described, according to the analytic formulas, through the coordinate matrix,

$$G=\begin{Vmatrix}X_{1_1} & Y_{1_1}\\ X_{1_2} & Y_{1_2}\\ \dots & \dots\\ X_{1_n} & Y_{1_n}\end{Vmatrix}, \quad (1)$$

thus, the distance between two successive points M_i, M_{i+1}, is small enough:

$$ds=\sqrt{\left(X_{1i+1}-x_{1i}\right)^2+\left(Y_{1i+1}-Y_{1i}\right)^2}\le\varepsilon, \quad (2)$$

$\varepsilon=1\cdot10^{-3}$mm.

We define βi the angle of inclination of the elementary segment, $tg\beta_i=\frac{\left|Y_{1i+1}-Y_{1i}\right|}{\left|X_{1i+1}-X_{1i}\right|}$, (3)

see Figure 2.

Table 2. *Analytic model of transverse profile of male rotor*

Sg.	Family of profiles	Meshing condition	Variable parameters
$\overset{\frown}{AB}$	$\begin{cases} X_1 = R_0 \cdot \cos(\psi - \varphi_1) + (R_{r_1} - c_0) \cdot \cos\varphi_1 + \\ + R_{r_1} \cdot \varphi_1 \cdot \sin\varphi_1; \\ Y_1 = -R_0 \cdot \sin(\psi - \varphi_1) + (R_{r_1} - c_0) \cdot \sin\varphi_1 - \\ - R_{r_1} \cdot \varphi_1 \cdot \cos\varphi_1; \end{cases}$	$\varphi_1 = -\frac{c_0}{R_{r1}} \text{tg}\psi$	$\psi_{min}=0$; ψ_{max}=constr.
$\overline{BC}$	$\begin{cases} X_1 = u \cdot \sin(\varphi_1 - \psi_{max}) + (R_{r_1} + \xi_B) \cdot \cos\varphi_1 + \\ + (R_{r_1} \cdot \varphi_1 + \eta_B) \cdot \sin\varphi_1; \\ Y_1 = -u \cdot \cos(\varphi_1 - \psi_{max}) - (R_{r_1} + \xi_B) \cdot \sin\varphi_1 + \\ + (R_{r_1} \cdot \varphi_1 + \eta_B) \cdot \cos\varphi_1; \end{cases}$	$\varphi_1 = \frac{-\frac{u}{\cos\psi_{max}} + \xi_B \cdot \text{tg}\psi_{max} - \eta_B}{R_{r_1}}$	$u_{min}=0$; u_{max}=constr. $\beta = \frac{\pi}{2} - \psi_{max}$
$\overset{\frown}{CD}$	$\begin{cases} X_1 = -r_0 \cdot \cos(\varphi_1 - \nu) + (R_{r_1} + \xi_{0_1}) \cdot \cos\varphi_1 - \\ - (-R_{r_1} \cdot \varphi_1 + \eta_{0_1}) \cdot \sin\varphi_1; \\ Y_1 = -r_0 \cdot \sin(\varphi_1 - \nu) + (R_{r_1} + \xi_{0_1}) \cdot \sin\varphi_1 + \\ + (-R_{r1} \cdot \varphi_1 + \eta_{0_1}) \cdot \cos\varphi_1;. \end{cases}$	$\varphi_1 = \frac{\xi_{0_1} \cdot \text{tg}\nu + \eta_{0_1}}{R_{r_1}}$	$\upsilon_{min}=0$; $\upsilon_{max} = \frac{\pi}{2} - \beta$
$\overset{\frown}{EF}$	$\begin{cases} X_1 = -r_0 \cdot \cos(\nu_1 + \varphi_1) + (R_{r_1} + \xi_{0_2}) \cdot \cos\varphi_1 + \\ + (R_{r_1} \cdot \varphi_1 - \eta_{0_2}) \cdot \sin\varphi_1; \\ Y_1 = -r_0 \cdot \sin(\nu_1 + \varphi_1) - (R_{r_1} + \xi_{0_2}) \cdot \sin\varphi_1 + \\ + (R_{r_1} \cdot \varphi_1 + \eta_{0_2}) \cdot \cos\varphi_1; \end{cases}$	$\varphi_1 = \frac{\xi_{0_2} \cdot \text{tg}\nu_1 + \eta_{0_2}}{R_{r_1}}$	$\upsilon_{1min}=0$; $\upsilon_{1max} = \frac{\pi}{2} - \beta_1$
$\overline{FG}$	$\begin{cases} X_1 = u_1 \cdot \cos(\varphi_1 - \beta_1) + (R_{r_1} + \xi_F) \cdot \cos\varphi_1 - \\ - (-R_{r_1} \cdot \varphi_1 + \eta_F) \cdot \sin\varphi_1; \\ Y_1 = u_1 \cdot \sin(\varphi_1 - \beta_1) + (R_{r_1} + \xi_F) \cdot \sin\varphi_1 + \\ + (-R_{r_1} \cdot \varphi_1 + \eta_F) \cdot \cos\varphi_1; \end{cases}$	$\varphi_1 = \frac{-\frac{u_1}{\sin\beta_1} + \xi_F \cdot \text{ctg}\beta_1 + \eta_F}{R_{r_1}}$	$u_{1min}=0$; u_{1max}=constr.
$\overset{\frown}{AH}$	$\begin{cases} X_1 = (\xi(\lambda) + R_{r1}) \cdot \cos\varphi_1 - \\ - (\eta(\lambda) - R_{r1} \cdot \varphi_1) \cdot \sin\varphi_1; \\ Y_1 = -(\xi(\lambda) - R_{r1}) \cdot \sin\varphi_1 + \\ + (\eta(\lambda) - R_{r1} \cdot \varphi_1) \cdot \cos\varphi_1; \end{cases}$	$\frac{\dot{X}_{1_{\lambda_1}}}{\dot{X}_{1_{\varphi_1}}} = \frac{\dot{Y}_{1_{\lambda_1}}}{\dot{Y}_{1_{\varphi_1}}}$	λ_1, λ_2
$\overset{\frown}{GH}$	$\begin{cases} X_1 = (\xi(\lambda) + R_{r1}) \cdot \cos\varphi_1 - \\ - (\eta(\lambda) - R_{r1} \cdot \varphi_1) \cdot \sin\varphi_1; \\ Y_1 = -(\xi(\lambda) - R_{r1}) \cdot \sin\varphi_1 + \\ + (\eta(\lambda) - R_{r1} \cdot \varphi_1) \cdot \cos\varphi_1; \end{cases}$	$\frac{\dot{X}_{1_{\lambda_2}}}{\dot{X}_{1_{\varphi_1}}} = \frac{\dot{Y}_{1_{\lambda_2}}}{\dot{Y}_{1_{\varphi_1}}}$	λ_1, λ_2

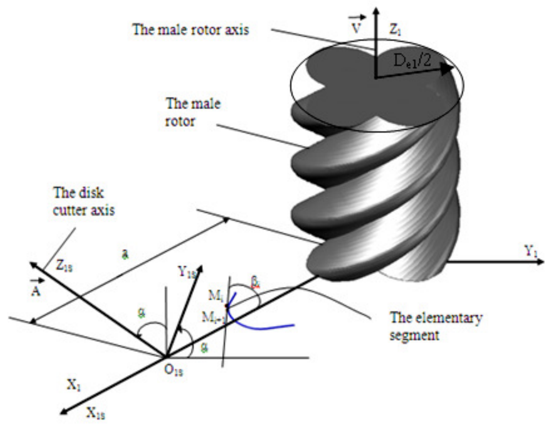

Fig. 2. *The helicoidal surfaces of male rotor; coordinates system*

To express the segment M_iM_{i+1}:

$$M_iM_{i+1}\left|\begin{array}{l} X_1 = X_{1i} + \lambda\cdot\cos\beta_i; \\ Y_1 = Y_{1i} + \lambda\cdot\sin\beta_i, \end{array}\right. \quad (4)$$

with $\lambda_{min} = 0$; $\lambda_{max} = d_S$, see (2).

We imagine an elementary helicoidal surface, described by the coordinates transformation as follows:

$$\left\|\begin{array}{l} X_1 \\ Y_1 \\ Z_1 \end{array}\right\| = \omega_3^T(\theta_1)\cdot\left\|\begin{array}{l} X_{1i} \\ Y_{1i} \\ 0 \end{array}\right\| + \left\|\begin{array}{l} 0 \\ 0 \\ p_1\cdot\theta_1 \end{array}\right\| \quad (5)$$

right helix, the helicoidal parameter p_1 and θ_1 the variable parameter.

The surfaces assembly (5) (i=1...n), represents an accurate substitution of the male rotor flank, corresponding to AB, BC, etc, see Table 2.

Obviously, the normal to the helicoidal elementary surface (5) can be written as follows:

$$\vec{N}_\Sigma = \vec{T}_{M_iM_{i+1}} \times \vec{T}_{M_i} \quad (6)$$

where

$$\vec{T}_{M_i} = \frac{dX_1}{d\theta_1}\cdot\vec{i} + \frac{dY_1}{d\theta_1}\cdot\vec{j} + p_1\cdot\vec{k}, \quad (7)$$

$$\vec{T}_{M_iM_{i+1}} = \cos\beta_i\cdot\vec{i} + \sin\beta_i\cdot\vec{j}. \quad (8)$$

The normal to the elementary helicoidal surface is calculated as follows:

$$\vec{N}_\Sigma = \left|\begin{array}{ccc} \vec{i} & \vec{j} & \vec{k} \\ -X_{1i}\sin\theta_1 - Y_{1i}\cos\theta_1 & X_{1i}\cos\theta_1 - Y_{1i}\sin\theta_1 & p_1 \\ \cos\beta_i & \sin\beta_i & 0 \end{array}\right|, (9)$$

or:

$$\vec{N}_\Sigma = N_{X_1}\cdot\vec{i} + N_{Y_1}\cdot\vec{j} + N_{Z_1}\cdot\vec{k}, \quad (10)$$

by the definitions:

$$\left\{\begin{array}{l} N_{X_1} = -p_1\cdot\sin\beta_i\ ; \\ N_{Y_2} = p_1\cdot\cos\beta_i\ ; \\ N_{Z_2} = \sin\beta_i\cdot\left[-X_{1_i}\cdot\sin\theta_1 - Y_{1_i}\cdot\cos\theta_1\right] - \\ -\cos\beta_i\cdot\left[X_{1_i}\cdot\cos\theta_1 - Y_{1_i}\cdot\sin\theta_1\right]. \end{array}\right. \quad (11)$$

3. Profiling the disk cutter — algorithm

The axis position of disk cutter, see Figure 2, is defined:

$$\vec{A} = -\sin\alpha\cdot\vec{j} + \cos\alpha\cdot\vec{k} \quad (12)$$

and the amount of the angle α,

$$tg\alpha = \frac{2\pi\cdot p_1}{\pi\cdot D_{e1}} = \frac{2\cdot p_1}{D_{e1}}, \quad (13)$$

where p_1 is the helicoidally parameter and De_1 represents the outlet diameter of male rotor.

Thus, the condition of characteristic curve determination on the elementary helicoidally surfaces becomes

$$\left(\vec{N}_\Sigma, \vec{A}, \vec{r}_2\right) = 0, \quad (14)$$

where:

$$\begin{array}{l} \vec{r}_1 = \left[X_{1i}\cdot\cos\theta_1 - Y_{1i}\cdot\sin\theta_1 - a\right]\cdot\vec{i} + \\ + \left[X_{1i}\cdot\sin\theta_1 + Y_{1i}\cdot\cos\theta_1\right]\cdot\vec{j} + p_1\cdot\theta_1\cdot\vec{k} \end{array}, \quad (15)$$

$-X_1$, Y_1 defined by (5);

a - the amount of the inlet radius of male rotor and outlet radius of disk cutter, convenient to be technologically determined.

The envelope condition becomes:

$$\left(\vec{N},\vec{A},\vec{r}\right) = \left|\begin{array}{ccc} (X_{1i}\cdot\cos\theta_1 - Y_{1i}\cdot\sin\theta_1 - a) & (X_{1i}\cdot\sin\theta_1 + Y_{1i}\cdot\cos\theta_1) & +p_1\cdot\theta_1 \\ -p_1\cdot\sin\beta_i & p_1\cdot\cos\beta_i & (X_{1i}\cdot\cos(\theta_1-\beta_i) + Y_{1i}\cdot\sin(\theta_1-\beta_i)) \\ -\sin\alpha & \cos\alpha & 0 \end{array}\right| \le \varepsilon, \quad (16)$$

ε: ($1\text{x}10^{-3}$mm).

The points belonging to the elementary helical surface, and fulfilling the meshing condition (16), represents the characteristic curve - the contact curve between helicoidal surfaces and primary peripheral surface of disk cutter. It can be expressed as the vector,

$$X_1^c = \left\{X_{1_i}^c \quad Y_{1_i}^c \quad Z_{1_i}^c\right\}^T, \quad (i=1...m)\cdot \quad (17)$$

Changing the coordinates system:

$$X_{1S} = \alpha \cdot \left(X_1 - a \right) \; ;$$

$$\alpha = \begin{Vmatrix} 1 & 0 & 0 \\ 0 & \cos\alpha & \sin\alpha \\ 0 & -\sin\alpha & \cos\alpha \end{Vmatrix}; \; a = \begin{Vmatrix} a \\ 0 \\ 0 \end{Vmatrix}, \qquad (18)$$

is obtained the expression of the characteristic curve in the system of disk cutter $X_{1S}Y_{1S}Z_{1S}$, see Figure 3:

$$\begin{cases} X_{1S} = X_{li}^{c} - a; \\ Y_{1S} = Y_{li}^{c} \cdot \cos\alpha + Z_{li}^{c} \cdot \sin\alpha; \\ Z_{1S} = -Y_{li}^{c} \cdot \sin\alpha + Z_{li}^{c} \cdot \cos\alpha. \end{cases} \qquad (19)$$

$i = (1....m)$.

The axial section of the disk cutter is obtained:

$$\begin{cases} H = -Y_{li}^{C} \cdot \sin\alpha + Z_{li}^{C} \cdot \cos\alpha; \\ R = \sqrt{\left[X_{li}^{C} - a \right]^2 + \left[Y_{li}^{C} \cdot \cos\alpha + Z_{li}^{C} \cdot \sin\alpha \right]^2} \end{cases} \qquad (20)$$

$i = (1....m)$.

According to this algorithm, all the surface constituents of male rotor corresponding to Table 2, can be solved.

4. Numerical examples

We present two frontal applications, different constructive solutions.

In Table 4 and Figure 3 are described the axial section coordinates of disk cutter for the male rotor.

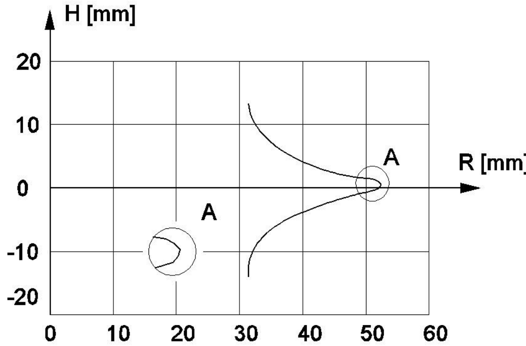

Fig. 3. *Male rotor – the tooth profile of disk cutter*

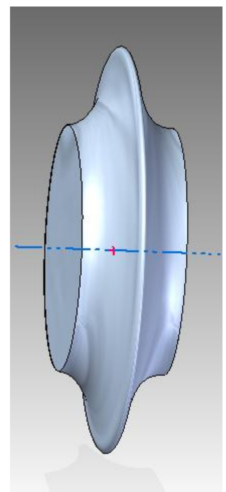

Fig. 4. *The solid of disk cutter for male rotor*

First application (screw compressor, ratio 4/6)

Table 3. *The constructive data of the rack generating, (see Figure 2)*

R_0 [mm]	r_0 [mm]	u_{max}[mm]	$\psi_{max}[^0]$	$\upsilon_{max}[^0]$	υ_{1max} $[^0]$	u_{1max}[mm]	L_p[mm]	c_0[mm]	Rr_2[mm]
22.000	1.100	10.300	63.400	63.400	58.285	6.451	50.265	4.000	32.000

Table 4. *The axial profile of disk cutter coordinates of male rotor*

Nr. crt.	R [mm]	H [mm]	Nr. crt.	R [mm]	H [mm]	Nr. crt.	R [mm]	H [mm]
1	31.398	-13.952	**41**	47.071	-1.449	**81**	37.437	5.413
2	31.366	-13.408	**42**	47.598	-1.306	**82**	36.974	5.701
3	31.369	-12.863	**43**	48.126	-1.171	**83**	36.516	5.997
4	31.408	-12.320	**44**	48.654	-1.036	**84**	36.069	6.309
5	31.483	-11.780	**45**	49.185	-0.914	**85**	35.629	6.630
6	31.595	-11.247	**46**	49.717	-0.793	**86**	35.199	6.966
7	31.751	-10.725	**47**	50.248	-0.670	**87**	34.781	7.315
8	31.952	-10.218	**48**	50.777	-0.536	**88**	34.373	7.677
9	32.186	-9.727	**49**	51.305	-0.402	**89**	33.982	8.057
10	32.449	-9.249	**50**	51.805	-0.224	**90**	33.600	8.445
11	32.761	-8.802	**51**	52.149	0.199	**91**	33.247	8.861
12	33.091	-8.369	**52**	52.279	0.604	**92**	32.906	9.286
13	33.448	-7.957	**53**	51.868	0.962	**93**	32.589	9.729

14	33.831	-7.570	**54**	51.427	1.258	**94**	32.305	10.194
15	34.226	-7.194	**55**	50.889	1.342	**95**	32.045	10.673
16	34.648	-6.849	**56**	50.350	1.426	**96**	31.819	11.169
17	35.074	-6.509	**57**	49.811	1.508	**97**	31.642	11.684
18	35.521	-6.197	**58**	49.269	1.563	**98**	31.506	12.211
19	35.972	-5.890	**59**	48.726	1.617	**99**	31.413	12.748
20	36.436	-5.606	**60**	48.186	1.693	**100**	31.370	13.291

The flank of male rotor is a helicoidal cylindrical surface, constant step, right helix, helicoidal parameter p_1 and $a = R_S + R_{1int}$.

Table 5. *The geometrical constructive elements of the male rotor*

Rr_1 [mm]	$Rext_1$ [mm]	a [mm]	p_1 [mm]	R_S [mm]	β [°]
32.0	53.0	100.0	19.099	68	57.205

Helical parameters are calculated with equation:

$$p_2 = \left(\frac{360^\circ}{300^\circ \cdot i} \cdot D_1 \right) \cdot \frac{1}{2 \cdot \pi} \qquad (21)$$

with i=4/6 or 3/5.

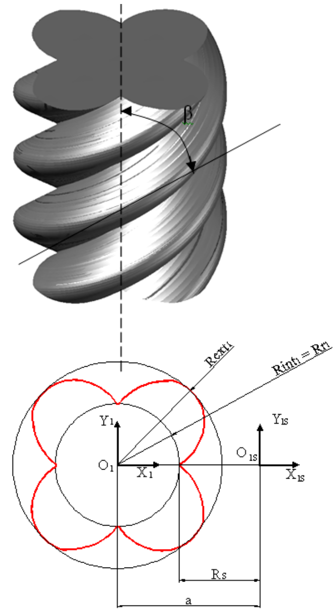

Fig. 5. *Solid model and the geometrical constructive elements of male rotor*

Second application (screw compressor, ratio 3/5)

Table 6. *The constructive data of the reference rack, (see Figure 2)*

R_0 [mm]	r_0 [mm]	u_{max}[mm]	$\psi_{max}[^0]$	$\upsilon_{max}[^0]$	υ_{1max} $[^0]$	u_{1max}[mm]	L_p[mm]	c_0[mm]	Rr_2[mm]
22.000	2.000	7.045	70.300	70.300	35.054	7.774	62.832	4.000	50.000

Table 7. *The axial profile of disk cutter coordinates of male rotor*

Nr. crt.	R [mm]	H [mm]	Nr. crt.	R [mm]	H [mm]	Nr. crt.	R [mm]	H [mm]
1	52.708	-19.046	**41**	68.092	-1.669	**81**	59.354	9.202
2	52.660	-18.427	**42**	68.611	-1.326	**82**	58.829	9.533
3	52.637	-17.806	**43**	69.121	-0.972	**83**	58.313	9.878
4	52.645	-17.185	**44**	69.618	-0.600	**84**	57.806	10.237
5	52.683	-16.566	**45**	70.105	-0.215	**85**	57.311	10.611
6	52.754	-15.949	**46**	70.594	0.168	**86**	56.827	11.001
⋮	⋮	⋮	⋮	⋮	⋮	⋮	⋮	⋮
16	55.311	-10.385	**56**	73.980	4.334	**96**	53.107	15.886
17	55.727	-9.924	**57**	73.428	4.615	**97**	52.917	16.477
18	56.163	-9.483	**58**	72.832	4.787	**98**	52.777	17.081
19	56.619	-9.061	**59**	72.220	4.888	**99**	52.692	17.696
20	57.091	-8.657	**60**	71.605	4.978	**100**	52.664	18.316

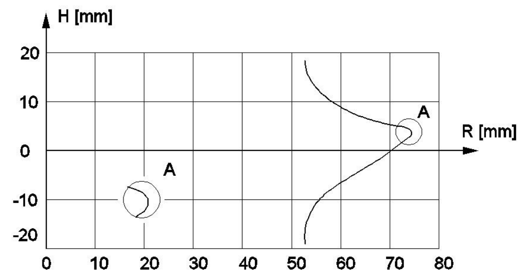

Fig. 6. *Male rotor – the tooth profile of disk cutter*

In Table 7 and Figure 6, are described the axial section coordinates of disk cutter for the male rotor.

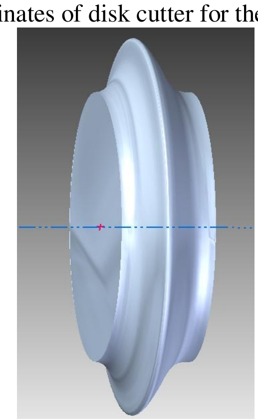

Fig. 8. *The solid of disk cutter for male rotor*

The flank of male rotor helicoidal surface is a helicoidal cylindrical surface, constant steep, right helix, helicoidal parameter p_1 and $a = R_s + R_{1int}$.

Table 5. *The geometrical constructive elements of male rotor*

Rr_1 [mm]	$Rext_1$ [mm]	a [mm]	p_1 [mm]	R_S [mm]	β [°]
30.0	52.0	100.0	20.245	70.0	57.318

5. Product software for determination of disk cutter profile

The product soft was elaborated with Sun Java Development Kit, according to the possibility of transverse profile of helicoidal surfaces to be approximated by Bézier polynomial superior degree.

The product allows generating the helicoidal surfaces of screw rotors; using the specific enveloping condition, see Table 1 and relation (20), it is possible to calculate the axial section of disk cutter, mutually enveloping the helicoidal surfaces, constant step, representing the grove between two successive lobes, male and female. The tool relative position was defined taking into account the present algorithm.

The flank corresponding to rotors generator, AB, BC, CD, etc. (see Figure 2), can be approximated by superior degree polynomial, thus the shape representation is very accurate.

This approach fits perfectly into the object Oriented Programming (00P) paradigm [11], [12].

Application description

In this section, application user interface will be described. The most important visual elements of the application are presented in Figure 9, as follows:

1 – select the type of helix generator profile;

2 – configure various parameters of the generating profile (in the case of "Measured points" a list of measured coordinates should be inserted);

3– select the tool type;

4 – configure a series of helix parameters: outer diameter, inner diameter and the pitch;

5 – update the helical surface displayed on the screen according to parameters and options selected above;

6 - characteristic curve on helical surface;

7 - the helical surface;

8 - helical surface origin and coordinates system;

9 - tool's axis and origin of coordinates system.

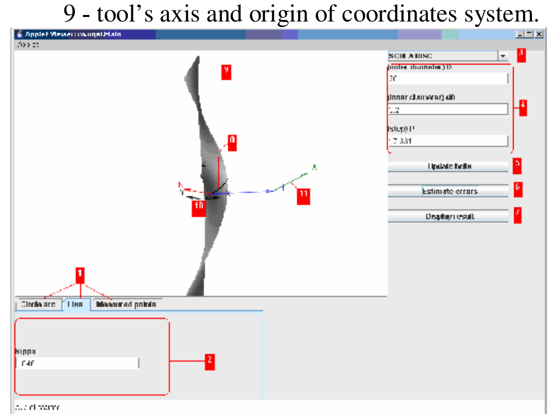

Fig. 9. *Application user interface*

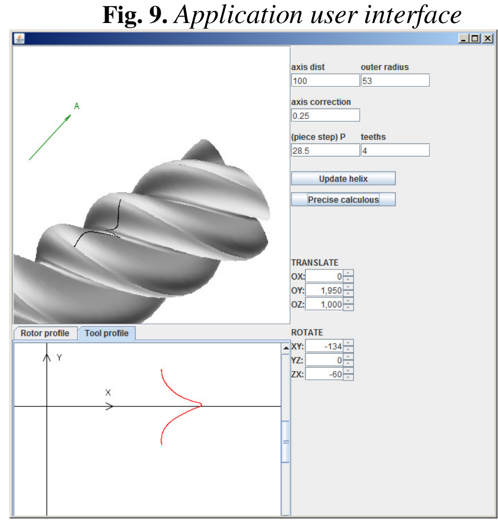

Fig. 10. *Male rotor disk cutter profile*

In Figure 10, it is presented the applet for the profiling of the disk cutter which generates the male rotor, the solid model of the worm and the characteristic curve onto its flanks.

In the applet, the significance of the coordinate axis *X* and *Y* corresponding to the equation (20):

$$X \equiv R; \quad Y \equiv H \tag{22}$$

5. Conclusions

This paper proposes a profiling method for the male rotor, setting the shape definition of the rack generating.

Using „The tangent method", the helicoidal surfaces of male rotors were substituted by elementary helicoidal surfaces, in order to decrease the analytic computation.

The numerical example of disk cutter profiling was presented, joined with a 3D solid model of primary peripheral surfaces of disk cutter, for diverse construction versions.

Acknowledgement

The authors gratefully acknowledge the financial support of the Romanian Ministry of Education, Research and Innovation through grant PN_II_ID_791/2008.

REFERENCES

[1]. Litvin, F. L., 1989, *Theory of Gearing*, NASA RP-1212 (AVSCOM 88-C-035), Washington, D.C.

[2] Oancea, N., *Surface generation through winding, Volume I, Fundamental Theorems*, 2004, "Dunărea de Jos" University publishing house, ISBN 973-627-106-4.

[3] Oancea, N., *Surface generation through winding, Volume II, Complementary Theorems*, 2004, "Dunărea de Jos" University publishing house, ISBN 973-627-106-4, ISBN 973-627-170-6.

[4] Teodor, V., 2010*, Contribution to the elaboration method for profiling tools-tools which generate by enwrapping*, Lambert Academic Publishing, ISBN 978-3-9433-8261-8.

[5] Zhou Z., 1992, *Computer Aided Design of a Twin Rotor Screw Refrigerant Compressor,* Proceedings of the 1992 International Compressor Engineering Conference at Purdue, West Lafayette, pp. 457–465.

[6] Litvin, F. L., and Feng, Pin-Hao, 1997, *Computerized Design, Generation, and Simulation of Meshing of Rotors of Screw Compressor*.

[7] Stosic N, Smith I. K, and Kovacevic A, 2002*: Optimization of Screw Compressor Design*, XVI International Compressor Engineering Conference at Purdue, July 2002.

[8] Stosic, N., Mujic, E., Smith, I.K., Kovacevic, A., *Profiling of Screw Compressor Rotors by Use Direct Digital Simulation*. International Compressor Engineering Conference at Purdue, July 2008.

[9] Tseng Ching-Huan, *Synthesis and Optimization for Rotor Profiles in Twin Rotor Screw Compressor*, Journal of Mechanical Design December 2000, Vol. 122, pp. 545.

[10] Stosic, N., Smith, I., Kovacevic, A., *Screw Compressors – Mathematical Modelling and Performance Calculation*. Springer, feb. 2005.

[11] *,** Sun Java Development Kit, http://java.sun.com/.

[12] *,** Java Tools and Libraries for the Advancement of Science, http://jscience.org/.

[13] Baicu, I., Oancea, N., *Profilarea sculelor prin modelare solida*, Editura TEHNICA-INFO, Chişinău, 2002, ISBN 9975-63-172-X.

Metodă pentru profilarea sculei disc destinate prelucrării rotoarelor din componența compresoarelor elicoidale; produs soft de profilare

—Rezumat—

Suprafețele active ale compresoarelor cu şurub sunt suprafețe elicoidale cilindrice cu pas constant. Aceste suprafețe sunt suprafețe complexe deoarece trebuie să îndeplinească o serie de condiții specifice.

În această lucrare se prezintă, în concordanță cu teoremele înfăşurării suprafețelor, o aplicație practică privind principiul înlocuirii generatoarelor elementare ale suprafețelor aparținând unui cuplu de suprafețe elicoidale descrise în mod discret, utilizând metoda tangentelor, în scopul de a determina forma frezei disc pentru generarea şurubului conducător.

În lucrare se prezintă şi un soft dedicat pentru profilarea acestor scule, dezvoltat în limbajul de programare Java.